DOI: 10.14621/ce.20160103

Small Scale PV-Power – On Site Use Maximization through Smart Heat Pump Control

Martin Felix Pichler[1]*, Alexander Arnitz[1], Markus Brychta[2], Andreas Heinz[1], René Rieberer[1]

[1]Graz University of Technology
Inffeldgasse 25/B, 8010 Graz, Austria; martin.pichler@tugraz.at, martin.pichler@gmx.eu
[2]University of Innsbruck

Abstract

Small scale grid-connected photovoltaic (PV) power plants may lead to unwanted disturbance to the electricity grid. In addition, low feed-in tariffs motivate the homeowner and operator of the PV plant to maximize the self-consumption.
A PV system in connection with a compression heat pump (HP) for heating (and cooling) purposes of a single family house equipped with some kind of thermal storage poses an interesting optimization problem in this context. Load management is possible through an intermediate thermal storage such as a simple water storage tank. However, in addition the building may comprise a thermally activated building system (TABS) such as a floor heating or an activated ceiling. Thermal storage capacity enables to maximize the utilization of PV-power to pre- or 'overheat' the water tank or the whole building, and at the same time the grid is prevented from overcharge and thus regulating (power) requirements are reduced.
This research investigates a system consisting of a small grid connected PV plant in connection with a HP charging a thermal storage. The load of the storage comprises domestic hot water draw offs and the space heating demand of a single family house. The main challenge is to maximize the PV-electricity self-consumption. The work presented herein is a preliminary study for a more complex system described in the introduction.

Keywords:	PV; Load change flexibility; Smart control, MPC; Thermal storage

Article history:	Received:	17 August 2015
	Revised:	10 September 2015
	Accepted:	29 January 2016

1. Introduction

Small scale grid-connected photovoltaic (PV) systems may represent an unwanted disturbance to the grid. In addition, low feed-in tariffs motivate the operators of the PV plant to maximize the self-consumption and minimize the consumption from the grid.

The volatile character of solar irradiance, typical for Central Europe, poses a challenge in terms of stability and control at grid level, if numerous small scale PV-systems potentially feed into the grid.

Assume a compression heat pump (HP) installed in a single family house for heating (and cooling) purposes. A predictive weather-forecast-utilizing control framework may be used for load management to maximize the PV-electricity self-consumption and prevent from overcharge at grid level and thus reduce regulating (power) requirements. This becomes possible, due to the relatively high thermal time constants of current standard buildings.

1.1. Short review on related research

Wimmer [1] has investigated the model predictive control (MPC) of a heat pump for a single family house with different approaches, but for constant compressor speed. Simulations have shown cost savings up to 13% – compared to a standard on/off controller – and an electricity consumption reduction up to 3.5%, on an annual base. Bianchi [2] continued this research and investigated an adaptive framework for the same application. Young [3] deals with the topic demand side management (DSM) with heat pumps for single family houses with floor heating – he found a prediction horizon of 24 h to outperform smaller horizons. The electrical load shifting potential of a smart heat pump has also been analyzed in Danny [4] with the finding of a

load shifting potential between 19% and 33%, however, the annual electricity consumption increased by approximately 9%.

1.2. The project TheBat

A research project dealing with a smart control of a HP-system in connection with a PV-system, for the purpose of space heating (SH) and domestic hot water (DHW) preparation is currently ongoing at Graz University of Technology and University of Innsbruck. The project "TheBat" comprises simulation, prototype test, and real hardware in the loop (HIL) tests.

Based on the building used in IEA SHC Task 44 (compare Figure 1) a reference building was defined. The scope is to analyse different concepts of thermal storage, also including the building mass itself. The gable roof is asymmetric, with a steeper south orientated part (26 m²) which can be easily used for solar applications. For further details see [5].

The original building was slightly adapted in order to meet the specific requirements of the project. The main differences are the implementation of thermally activated building systems on the ground level and the first floor. Three different building types were considered (see Table 1). The buildings RES 45 and OFF 45 will be investigated in connection with the HP-, PV-system operated by a model predictive control (MPC). The planned *actuating variables* are the HP-power (frequency) and valve positions to divide the heat supply to the storage and/or the building. *Controlled variables* are a storage tank- and the air-temperature in the building. The aim is to apply a linear MPC concept which requires a linear model for the thermal storage and the building dynamics. In addition, the expected PV-generated electricity must be estimated by given weather forecast data. Finally the HP-characteristic has to be modelled using a suitable approach.

Research presented herein focusses on three stages on the way to the final solution for the complex system. First, it deals with modelling related to PV-generated electricity, second, it covers the thermal storage tank modelling part, and finally this research reports on definitions made to evaluate the controller and the system performance.

2. Reference system and boundary conditions

The parametrization of a predictive controller, which means setting a reference trajectory, minimum and maximum bounds and weights for the actuated and controlled variable etc. requires certain simulation experiments to assure a reasonable control behavior. The reference system described in the following and the research reported in this manuscript is tailored to gain insight into the heat pump related MPC parametrization. Building related modelling for MPC purpose is not covered in this report.

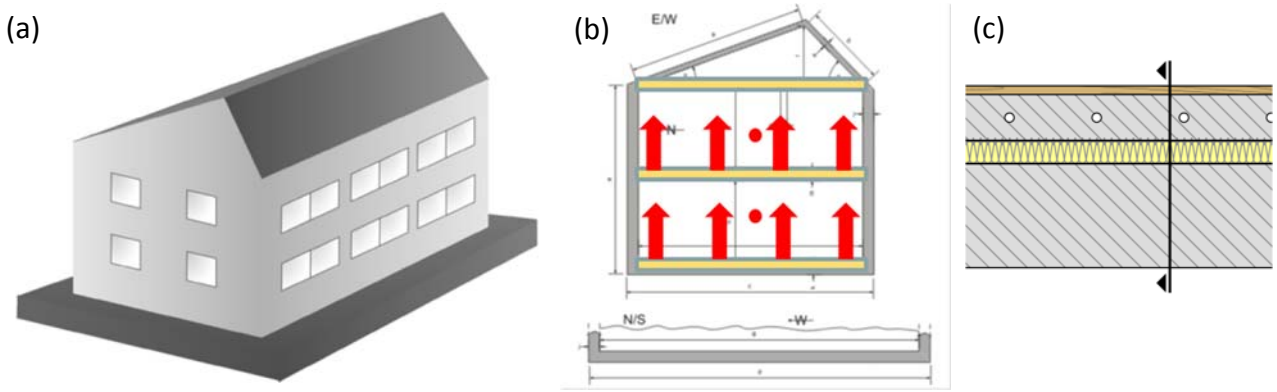

Figure 1: 3D view of the reference building (a), illustration of thermally activated floors (b), and related cross-section of the floor (c) [5]

Table 1 Characterization of the buildings investigated in the research project TheBat

Building Type	Usage	Heat demand approx.	U-Value Walls	U-Value ceiling (1st floor)
RES 45	Residential	45 kWh/(m² a)	0.29 W/(m² K)	0.69 W/(m² K)
OFF 45	Office	45 kWh/(m² a)	0.29 W/(m² K)	0.60 W/(m² K)
RES 15	Residential	15 kWh/(m² a)	0.18 W/(m² K)	1.27 W/(m² K)

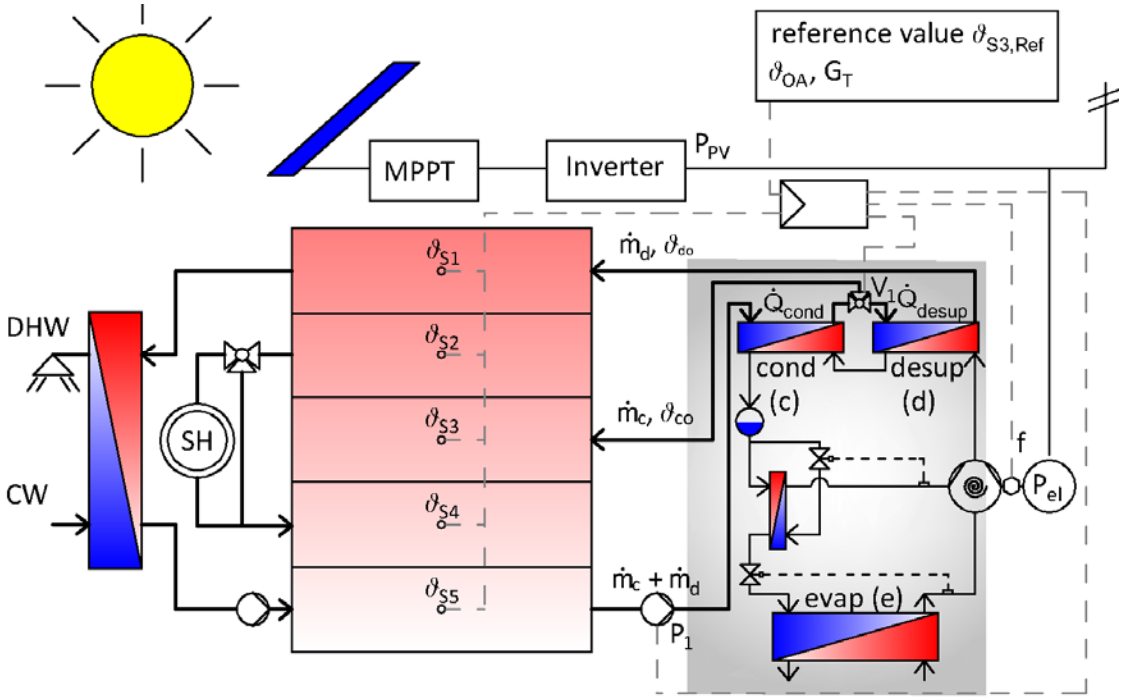

Figure 2: Scheme of the system controlled by the MPC. Abbreviations not explained in the further text: Domestic hot water (DHW), cold water (CW)

2.1. Hydraulic and electric scheme

This section introduces the reference simulation system illustrated in Figure 2. It consists of a heat pump (7 kW @B0W35), a thermal storage and a PV array. By contrast to the original system of the project TheBat, the SH demand is incorporated by means of a load profile, which acts on an increased thermal storage tank to mimic the thermal inertia of the building.

The ground is assumed to serve as a heat reservoir for the HP. The evaporator (e) supply temperature is assumed as constant 10 °C. The HP cycle consists of a scroll-compressor with variable speed (f) and an economizer which injects medium pressure vapor into the compressor. Heat delivery from the HP to the storage occurs via the condenser (c) which connects to the storage at half height and via the desuperheater (d) at the top. More details on the HP may be found in [6].

The thermal storage with a volume of 1.2 m³ represents the heat sink. It incorporates five equally spaced sensors to measure the temperature stratification (ϑ_{Si}). The counter flow heat exchanger for DHW preparation is connected at the top of the storage as is the desuperheater outlet of the HP. The SH connection is situated below these connections. The DHW and SH return flows are reinjected in the lower storage region.

During ordinary heat pump operation, the circulation pump (P_1) ensures a mass flow rate in order to reach a 5 K higher temperature at the outlet of the condenser ($\vartheta_{co} = \vartheta_{ci} + 5$ K). A share of this mass flow is diverted with the valve (V_1) to pass through the desuperheater, however, the bigger part is charged into the storage. The mass flow further heated in the desuperheater is adjusted such to reach the set outlet temperature ($\vartheta_{do,set} = \vartheta_{co} + 25$ K) – characteristic diagrams are utilized to determine the required mass flows.

2.2. PV power estimation and climate data

The suggested control scheme requires a model to estimate the PV power given a forecast time series for the solar irradiance. A few models with different degree of complexity may be found in literature – see [7-9]. These approaches are based on a method to derive PV electrical characteristics from generally provided test data, see [10]. The four-parameter model from Eckstein [7] is used in TRNSYS for annual simulations.

The approach, facilitated to estimate the expected PV power from irradiance for control purpose relies on a simple *efficiency model*, which is briefly described in the following – a detailed description may be found in [7] or [11].

The basic assumption of this approach is the existence of a maximum power point tracker (MPPT). This device assures an operation of the PV array, such that in the I-V graph, the area below the operating point becomes a maximum. Finally, the efficiency of the PV array is given as a function of the actual cell- and outside ambient-

temperature (ϑ_{oa}), and of irradiance on the aperture area (G_T). The cell temperature (ϑ_{cell}) may be approximated by an energy balance considering the incoming solar energy, the generated electricity and the dissipated heat energy. The formula is given by Eq. 1 with $\tau\alpha = 0.9$ as mean absorbance transmission constant, and U_L and $\eta_{MP,ref}$ being the heat loss coefficient and the efficiency at reference conditions, both derived from manufacturers data. As reference conditions Nominal Operating Cell Temperature (NOCT) conditions are used.

$$\vartheta_{cell} = \vartheta_{oa} + \frac{G_T\,(\tau\alpha)}{U_L}\left(1 - \frac{\eta_{MP,ref}}{(\tau\alpha)}\right) \quad (1)$$

Given $\vartheta_{\mathrm{cell}}$ the actual efficiency at MP is calculated using Eq. 2 with $U_{\mathrm{oc,ref}}$ and $I_{\mathrm{sc,ref}}$ characterizing the open circuit voltage and short circuit current and the μ's the according temperature coefficients at reference conditions. Figure 3 shows the relatively good approximation of $\eta_{MP}(\vartheta_{oa})$ and the maximum power for different irradiance values (G_T), when comparing the efficiency- against the four parameter model results.

$$\eta_{MP} = \eta_{MP,ref}\left(1 + \left(\frac{\mu_{Uoc}}{U_{oc,ref}} + \frac{\mu_{Isc}}{I_{sc,ref}}\right)\left(\vartheta_{cell} - \vartheta_{cell,ref}\right)\right) \quad (2)$$

The climate data set for simulation represents the conditions for Strasbourg, compare [5]. Although the PV array, with a total cell aperture area of 20.4 m² facing south at an angle of 45° is connected to the grid, its main purpose is to drive the HP.

3. Methods and performance indicators

Simulations conducted with TRNSYS [12] use a time step of 2 min. The maximization of the direct utilization of in situ generated PV electricity can be interpreted as a motivation for the advanced control strategy.

3.1. Base case scenario

Table 2 provides an overview for annual simulation results obtained with a standard hysteresis control. The values fit to a typical single family home. $G_{T,S,45°}$ is the total incident solar radiation on the inclined PV cell aperture area and W_{PV} the total PV generated electricity. W_{el} is the total compressor electricity demand, and Q_{cond} and Q_{desup} represent the heat delivered by the condenser and the desuperheater. Q_{DHW} and Q_{SH} give the hot water and the heating energy demand and $Q_{\mathrm{S,loss}}$ indicates the thermal storage losses. The total demand Q_{DHW} + Q_{SH} must be covered by the totally generated heat, Q_{cond} + Q_{desup}.

3.2. Predictive controller

The goal for the investigated predictive controller is to cover as much as possible of W_{el} with W_{PV}. The control is mostly concerned with temperatures being the controlled variables and thermal power or a related variable (compressor speed) being the actuating variable. The refrigerant cycle itself is not in focus of the research. The controller is implemented in MATLAB [13] and relies on *ideal forecast* data for the weather, meaning that the used prediction values match the simulation data. A (disturbance) *prediction* for the *DHW and SH* demand is *currently not incorporated*. The MPC is called every 10 minutes to update the power of the HP

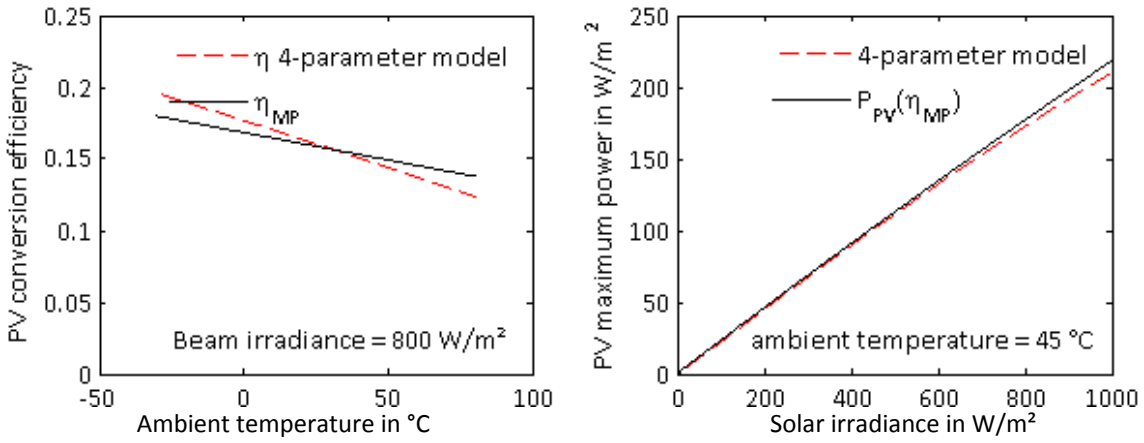

Figure 3: PV module efficiency as a function of the ambient temperature (left) and PV power as a function of the irradiance (right) – PV module Solarwatt 60P

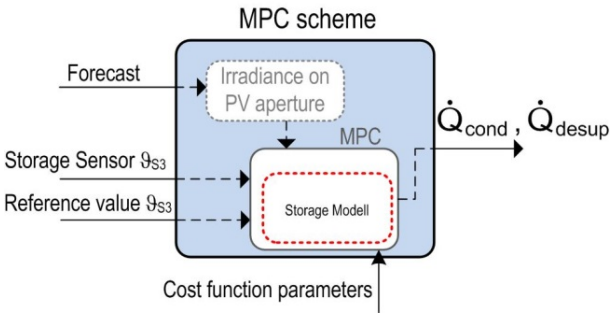

Figure 4: Overview of the predictive control scheme. The measured storage temperature provides feedback to the MPC

and the division into condenser and desuperheater heat flux. The general reference value for ϑ_{S3} is 50 °C.

3.3. Predictive controller

The principal compressor frequency control range is from approximately 30 Hz to 117 Hz. The heat pump coefficient of performance (COP, Eq. 3) depends mainly on the frequency, the condenser inlet temperature and the source temperature (assumed constant 10 °C).

For the classic reference case simulation the compressor frequency is set to 90 Hz constantly during HP operation. The HP turns on for $\vartheta_{S3} < 45\ °C$ and turns off at $\vartheta_{S3} > 50\ °C$. During MPC operation the compressor frequency is adjusted according to the required power.

3.4. Performance indicators

The HP coefficient of performance (COP) is given as the sum of heat flux delivered by the condenser and the desuperheater $(\dot{Q}_{cond} + \dot{Q}_{desup})$ divided by the required power to drive the compressor (P_{el}) and the pump P_1 ($P_{aux,el}$):

$$COP = \frac{\dot{Q}_{cond}+\dot{Q}_{desup}}{P_{el}+P_{aux,el}} \quad . \tag{3}$$

The main performance indicator is the *seasonal performance factor* (SPF) of the HP (Eq. 3a). It is defined as the totally delivered thermal energy $(Q_{cond} + Q_{desup})$ divided by the auxiliary (P_1) and compressor electr. consumption $(W_{el} + W_{aux,el})$ of the HP, during the same interval:

$$SPF = \frac{Q_{cond}+Q_{desup}}{W_{el}+W_{aux,el}} \quad . \tag{3a}$$

Concerning the control, a *controller performance related SPF* is defined (Eq. 4), which presents an interesting indicator for the HP control. It deviates from Eq. 3a only in the denominator. The integral represents the pure grid consumption due to HP operation. The sub index at the closing bracket indicates that only positive values are allowed, a negative value would mean feeding into the grid, which is not taken into consideration. A high SPF_{Ctr} indicates a good control concerning a high degree of electricity self-consumption:

$$SPF_{Ctr} = \frac{Q_{cond}+Q_{desup}}{\int_{0\,h}^{8760\,h}\left(P_{el}+P_{aux,el}-P_{PV}\cdot ON_{HP}\right)_{>0}\,dt} \quad . \tag{4}$$

Extending towards the whole system one may define a system specific SPF_{Ctr} (Eq. 5), which indicates the generated useful energy, for DHW and SH purpose $(Q_{DHW} + Q_{SH})$, per kWh of grid consumed electricity. This is the most interesting indicator at system level:

$$SPF_{Ctr,sys} = \frac{Q_{DHW}+Q_{SH}}{\int_{0\,h}^{8760\,h}\left(P_{el}+P_{aux,sys,el}-P_{PV}\cdot ON_{HP}\right)_{>0}\,dt} \quad . \tag{5}$$

The term $P_{aux,sys,el}$ incorporates the required power over all auxiliary devices of the system.

4. Simulation results for MPC- and Base-Case

The characteristic behavior of the MPC in comparison to the classic base case control is demonstrated by means of temperature and heat flux trajectories for seven sequential days.

Summer simulation results are depicted in Figure 5 and Figure 6. The smart MPC and the relatively low heat demand lead to HP operation only at times with PV power being available (Figure 5). For the MPC operated HP the COP at operation times is higher than for the classic control (Figure 6), compare also Table 3. However, this depends on the heat exchanger design and the compressor efficiency characteristic, which varies among HPs.

Winter simulation results look slightly different due to increased total heat demand compared to the summer; this is demonstrated by Figure 7 and Figure 8.

The MPC in winter is also characterized by HP operation at times where PV power is available. This PV-led operation causes overheating in the storage as visible in the top graph of Figure 7. However, by contrast to the summer, the HP is also operated at times where P_{PV}=0. Suddenly decreasing storage temperatures indicate SH- or DHW- heat demand. Sometimes (P_{el}+$P_{aux,el}$) is smaller than the available PV power, this indicates potential for improvement. The classic control depicted in Figure 8 leads to shorter HP operation intervals with increased power and the temperature trajectories show less variation.

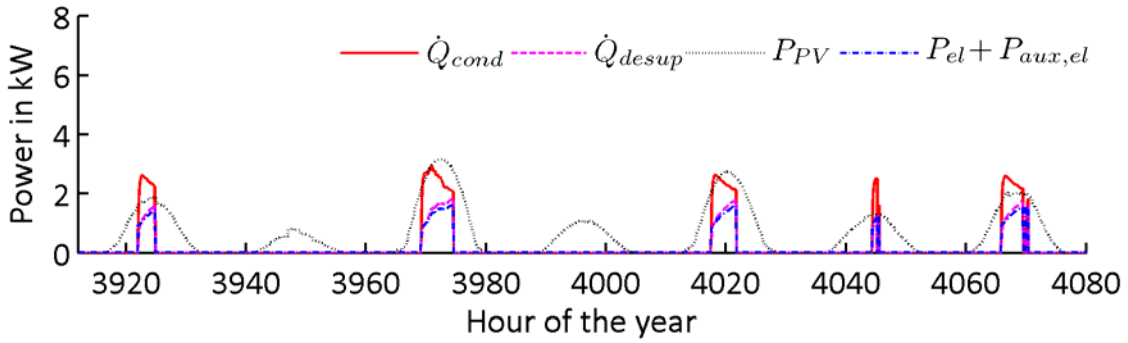

Figure 5: MPC simulation results for the heat fluxes and PV power for seven summer days

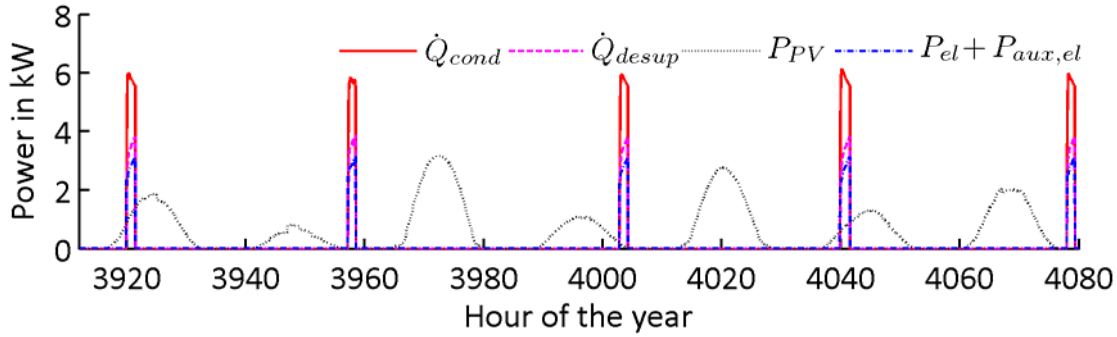

Figure 6: Classic control (base case) for the heat fluxes and PV power for seven summer days

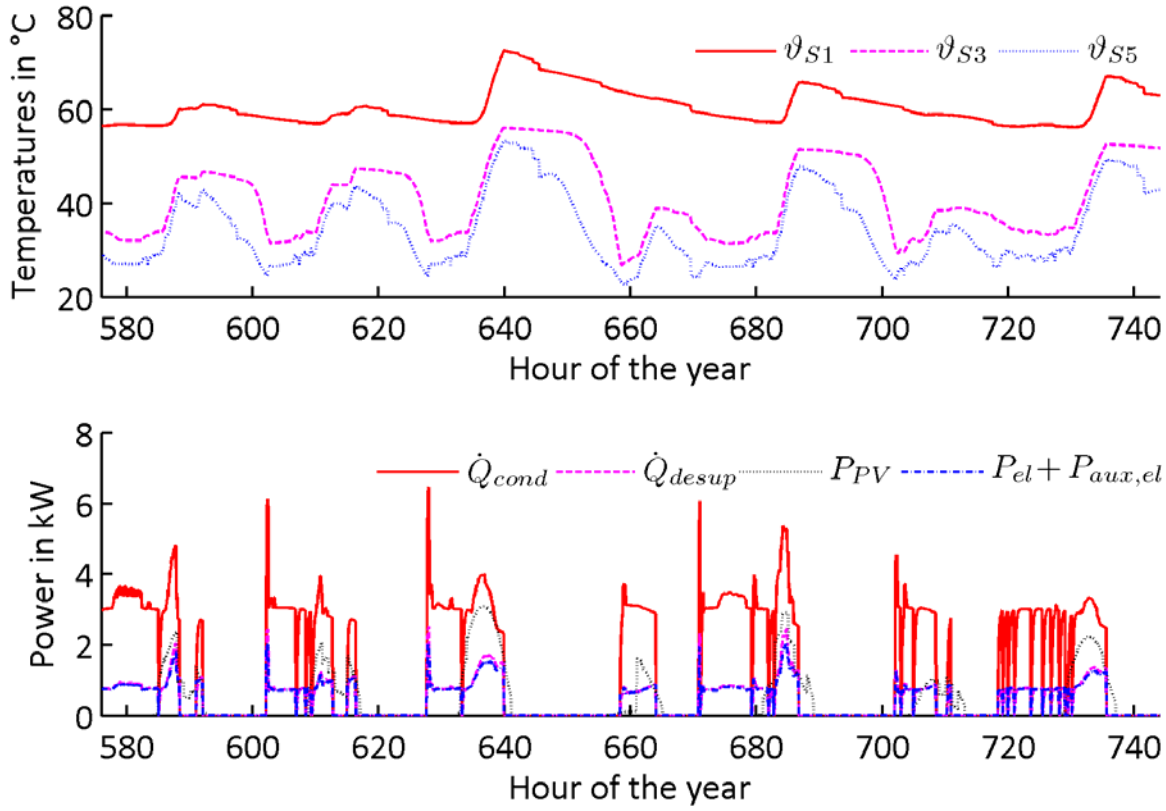

Figure 7: MPC results; the top graph shows the top, middle and bottom storage temperature, and the lower graph shows the relevant heat fluxes and PV power, for seven winter days

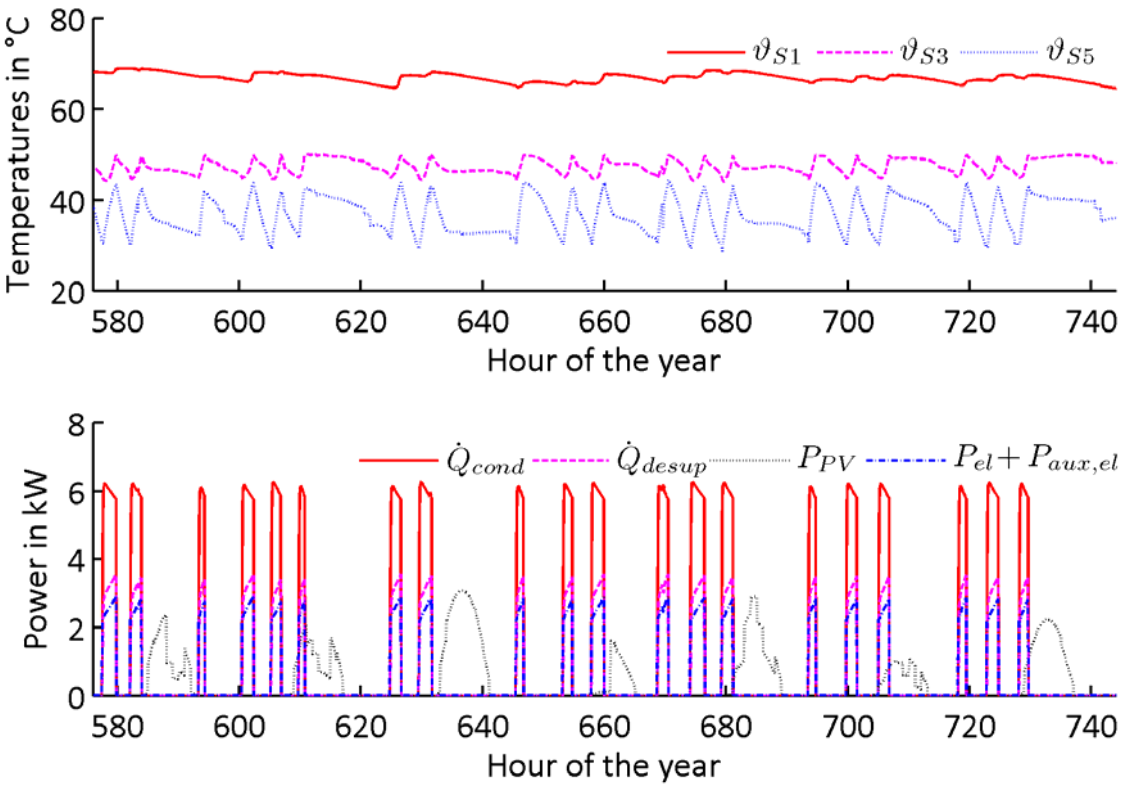

Figure 8: Classic control, base case results for top, middle and bottom storage temperature (top graph) and relevant heat fluxes and PV power (lower graph) for seven winter days

Table 2: Base case and MPC scenario simulation results.
Note: The specific PV power is with respect to the cell aperture area, and the DC/AC conversion efficiency is assumed 1

	$Quantity$	$G_{T,S,45°}$	W_{PV}	W_{el}	Q_{cond}	Q_{desup}	Q_{DHW}	Q_{SH}	$Q_{S,loss}$
Base Case	kWh	25264	4272	2689	6027	3236	2127	6475	640
	kWh/m^2_{PV}	1236	209	132	295	158	104	317	31
MPC	kWh	25264	4272	2352	6982	2363	2132	6464	744
	kWh/m^2_{cell}	1236	209	115	342	116	104	316	36

Table 3: Performance indicators for the base case and the MPC scenario

$Quantity$	SPF	SPF_{ctr}	$SPF_{ctr,ideal}$	$SPF_{ctr,sys}$	COP mean $\pm$ sigma	η_{PV} mean $\pm$ sigma
Base Case	3.38	3.66	5.24	3.30	3.38 ± 0.49	0.17 ± 0.01
MPC	3.77	7.80	10.75	6.73	3.92 ± 1.04	0.17 ± 0.01

4.1. Annual Results

Table 2 provides annual simulation results for relevant amounts of heat and generated electricity for both, the base case and the MPC case. The situation in terms of incident solar radiation ($G_{T,S,45°}$), PV output (W_{PV}), generated heat (Q_{cond}+Q_{desup}) and heat consumption (Q_{DHW} +Q_{SH}) is approximately the same for both cases.

The required electricity demand for the compressor (W_{el}) is higher for the base case since the compressor in that case operates constantly at 90 Hz for which the COP is mostly lower than the COP at MPC operation, where the dominant operation frequency is close to the lowest frequency approximately 35 Hz (compare COP values in Table 3, notice also the higher empirical standard deviation (σ) for the MPC case).

The significant "overheating" for the MPC case, as visible in the top graph of Fig. 7, leads to approximately 15% higher storage losses ($Q_{S,loss}$) for the MPC case.

The performance of the suggested MPC framework may be expressed by the control related SPF (SPF_{ctr}) defined by Eq. 4. This SPF indicates to which degree the HP uses the available PV electricity. The upper limit is given by $SPF_{ctr,ideal}$, which is an ideal theoretical value. This value is based on the assumption, that P_{el}+$P_{aux,el}$ – at times where available PV power overlaps with the HP operation time – is entirely provided by the PV plant. As Table 3 shows the control related SPF is much higher for the MPC case than for the base case. The number of 7.8 means that a consumption of 1 kWh_{el} from the grid, leads to 7.8 kWh of generated heat. The system and control related SPF ($SPF_{ctr,sys}$) shows that the effect concerning the whole system is smaller, which is mainly due to the increased storage losses.

5. Conclusion and future work

The self-consumption tailored MPC framework of the heat pump shows a relatively high degree of operation time during available PV power, leading to a SPF_{ctr} of 7.8 and a slightly smaller $SPF_{ctr,sys}$ of 6.73. These SPF's neglect the consumption of PV generated electricity. Young [3] found values ranging from 8.6 to 17.0 for a similar performance indicator as SPF_{ctr} is, but considering solar and wind generated electricity from the grid instead of purely on-site PV generated electricity.

Future work will focus on the extension and improvement of the MPC framework. This means incorporation of a heating demand prognosis through a building model, which entails also a further control variable (room air temperature). Further, the COP as a function of the compressor frequency of the HP will be incorporated into the MPC framework. In addition, several sensitivity analyses with respect to relevant sizing parameters will be conducted.

Acknowledgement

The project "The thermal battery in the smart grid in combination with heat pumps – an interaction optimization (TheBat)" is sponsored by the Austrian Climate and Energy Fund and conducted within the framework of the program „ENERGY MISSION AUSTRIA" (Project-Number 838657).

References

[1] Wimmer, R. W., Regelung einer Waermepumpenanlage mit Model Predictive Control (Model predictive control of a heat pump system), PhD thesis, ETH Zuerich, 2004.

[2] Bianchi, M. A., Adaptive Modellbasierte Praediktive Regelung einer Kleinwaerme-pumpenanlage (Adaptive model based predicitive control of a small scale heat pump system), PhD thesis, ETH Zuerich, 2006.

[3] Young, J. Y., Demand-side-management with heat pumps for single family houses, *Proceedings of BS2013*, 13th Conference of International Building Performance Simulation Association, Chambery, France, 2013.

[4] Danny, G., Wapler, J., Miara, M., Simulation and analysis of demand-side-management effects on operating behavior and efficiency of heat pumps, *11th IEA Heat Pump Conference Proceedings*, Montreal, Quebec, 2014.

[5] Dott, R., Haller, M. Y., Ruschenburg, J., Ochs, F. & Bony, J., The Reference Framework for System Simulations of the IEA SHC Task 44 / HPP Annex 38 Part A: General Simulation Boundary Conditions; Part B: Buildings and Space Heat Load, Technical report, IEA, 2013.

[6] Hengel, F., Heinz, A., Rieberer, R., Analysis of an air source heat pump system with speed controlled compressor and vapor injection, *Applied Thermal Engineering*, in Review, 2014.

[7] Eckstein, J. H., Detailed modelling of photovoltaic system components, Master's thesis, University of Wisconsin – Madison, 1990.

[8] Fry, B., Simulation of grid tied building integrated photovoltaic systems, Master's thesis, University of Wisconsin – Madison, 1998.

[9] Soto, W. D., Klein, S. & Beckman, W., Improvement and validation of a model for

photovoltaic array performance, *Solar Energy 80(1),* 78 – 88, 2006.

[10] Townsend, T., A Method for Estimating the Long-Term Performance of Direct-Coupled Photovoltaic Systems, Master's thesis, University of Wisconsin – Madison, 1989.

[11] Duffie, J. A., Beckman, W., *Solar Engineering of Thermal Processes*, Wiley, 2006.

[12] Klein, S., Beckman, W., Mitchell, J., Duffie, et al., A TRaNsient SYstems Simulation Program – TRNSYS 17.00.0019, Manual, Solar Energy Laboratory, University of Wisconsin-Madison, 2010.

[13] Bemporad, A., Morari, M., Ricker, N. Lawrance, Model Predictice Control Toolbox Users's Guide V3.2, Release 2010a, Mathworks, Natick, MA, 2010.